

CIRCULAR ARRAY OF COAXIALLY-FED MONOPOLE ELEMENTS
IN A PARALLEL PLATE WAVEGUIDE - THEORY

Boris Tomasic
Rome Air Development Center
Electromagnetic Sciences Division
Hanscom AFB, MASS. 01731, USA

ABSTRACT: The performance of a circular array of coaxially-fed monopole elements radiating into an infinite parallel plate region is analyzed. An outline of analysis for the phase-sequence input admittance, element pattern and coupling coefficients is presented. The characteristic features of the patterns are described and their dependence on array and element geometry is discussed.

INTRODUCTION: Circular ring arrays of coaxially-fed monopole elements between two circular parallel plates with E-plane (radial) flare are appealing for applications requiring scanning of a uniform beam 360 degrees in azimuth. The coaxial monopole element is an attractive choice for an array radiator due to its simplicity, high power, low cost, commercial availability and reasonably wide bandwidth. For high antenna performance, an accurate knowledge of the radiation properties of the element in the array environment is essential.

In this paper, a circular-ring array of uniformly spaced coaxial monopoles placed around conducting cylinder in an infinite parallel plate region is investigated to establish the array element admittance and pattern characteristics. We outline the steps in the analysis for the phase-sequence active admittance, the far-field in a parallel plate waveguide due to a singly excited coaxially-fed monopole element in a circular array environment, and the coupling coefficients. The phase-sequence admittances and the coupling coefficients provide information for the element design, while the element pattern is needed to predict radiation field of the array.

The analysis takes into account the geometry of the feed system. The probe current is assumed to have only an axial component and no angular variation. This approximation is justified since the probe radius is small compared to the wavelength. Furthermore, the analysis assumes that the field distribution in the coaxial aperture is that of the TEM mode in the coaxial feed-line which is consistent with the angularly uniform probe current density.

THE ARRAY MODEL: Figures 1 and 2 show the model under consideration. The top plate of the infinite parallel plate waveguide is partially removed to display the section of the array. The circular-ring array of coaxially-fed monopoles of length l is in a parallel plate waveguide of height h (only the TEM mode propagates since $h < \lambda/2$). The ring, of radius B , contain N equispaced identical monopoles each located coaxially a distance s above a perfectly conducting circular cylindrical surface of radius A . The probe radius is $a \ll \lambda$ while the inner and outer radii of the coaxial lines are a and b , respectively.

OUTLINE OF ANALYSIS: The procedure for the determination of phase-sequence input admittance $Y(\nu)$ is based on [1]. All elements are initially excited with aperture voltages of equal amplitude V_0 and progressive phase according to $\exp(-j2\pi\nu p/N)$ where $\nu = 0, 1, \dots, N-1$ is the angular wave number and $p = 0, 1, \dots, N-1$ is the element serial number. The $p=0$ element is designated as the reference element.

To evaluate $Y(\nu)$, an integral equation is formulated for the unknown probe current via the requirement that the total axial electric field $E_z(\underline{r};\nu)$ vanishes on the probe surface. The $E_z(\underline{r};\nu)$ is produced by all the ν -th phase-sequence probe currents as well as by the known equivalent magnetic ring distributions in the coaxial apertures. The procedure is carried out in a number of steps:

1. $E_z(\underline{r};\nu)$ is regarded as a superposition of two contributions, i.e.,

$$E_z(\underline{r};\nu) = E_z^{\text{inc}}(\underline{r};\nu) + E_z^{\text{S}}(\underline{r};\nu) \quad (1)$$

where the particular solution E_z^{inc} is due to the ring array of the exact, but yet unknown phase-sequence probe currents and the surrounding, known phase-sequence magnetic ring sources in an infinitely extended parallel plate waveguide in the absence of conducting cylinder ($A \rightarrow 0$). The E_z^{S} is a homogeneous (source free) solution in a unit cell such that

$$E_z(A, \phi, z; \nu) = 0. \quad (2)$$

2. Expressions are obtained for $E_{z0}(\hat{\rho}, z)$, due to an isolated (single) reference probe current and a concentric magnetic ring source in an infinite parallel plate waveguide.

3. Now, referring to Fig. 3 for an observation point $P(\rho < B, \phi, z)$, $E_z^{\text{inc}}(\underline{r};\nu)$ is obtained as a superposition of the N individual probe currents and the associated concentric magnetic ring source contributions centered at $\underline{\rho}_p$.

4. Using the Addition Theorem for Hankel functions, $E_z^{\text{inc}}(\underline{r};\nu)$ is expanded in terms of the Floquet modes in a radial unit cell.

5. The homogeneous solution $E_z^{\text{S}}(\underline{r};\nu)$ is formed in terms of Floquet modes in the radial unit cell where expansion coefficients are determined via (2) and step 4.

6. For an observation point $P(a, \hat{\phi}, z)$ on the reference probe $p=0$, as indicated in (1), $E_z(\underline{r};\nu)$ is obtained as a superposition of N isolated (single) probe-aperture combination E_z^{inc} , centered at $\underline{\rho}_p$ ($p=0, 1, \dots, N-1$), and the homogeneous solution E_z^{S} given in step 5.

7. To apply $E_z(\underline{r};\nu)=0$ on the probe surface, E_z^{inc} due to $p > 1$ and E_z^{S} are re-expanded about a cylindrical axis centered at the reference element. In view of the rotationally symmetric reference probe current distribution, only terms with no angular variation need be considered.

8. Steps 1 to 7 yield the desired integral equation for probe current. Application of Galerkin's procedure yields a set of linear inhomogeneous equations for the determination of the unknown probe expansion coefficients.

10. Having solved for the probe current, then following the procedure indicated in steps 1 to 6 the magnetic field in the aperture $H_{\phi}^{\wedge}(\hat{\rho}, z=0^{\dagger})$ is determined, where $a < \hat{\rho} \leq b$.

11. Continuity of H_{ϕ}^{\wedge} is imposed across the aperture which yields the expression for the ν -th phase-sequence input admittance. The relation for $Y(\nu)$ will be given at the presentation.

12. The far-zone field $E_z^{(e)}$ due to a singly excited element in an array environment is

$$E_z^{(e)}(\underline{\rho}) = \frac{1}{N} \sum_{\nu=0}^{N-1} E_z(\underline{\rho};\nu) \quad (3)$$

where $E_z(\underline{\rho};\nu)$ is the total far-field of the active array (for all elements excited with phase progression $\exp(-j2\pi\nu\rho/N)$) at an observation point $\underline{\rho} = \underline{x}_0 X + \underline{y}_0 Y$. $E_z(\underline{\rho};\nu)$ can be determined following procedure indicated in steps 1 to 6 in previous section where now $\rho > B$.

13. Coupling coefficients between reference $p=0$ and p -th elements are determined via

$$s_{0p} = s_p = \frac{1}{N} \sum_{u=0}^{N-1} \Gamma(z=0^-; u) e^{-j \frac{2\pi}{N} u p}, \quad (p = 0, 1, \dots, N-1). \quad (4)$$

The phase sequence reflection coefficients at the aperture plane are given in terms of $Y(u)$ and characteristic admittance of the coaxial feed line.

NUMERICAL RESULTS AND DISCUSSION: Based on the above analysis, a computer program was generated for evaluation of the phase-sequence active input admittances, the phase-sequence active reflection coefficients, the element patterns and of the coupling coefficients. In order to maximize the broadside element gain, a matching network appropriate to in-phase excitation of all monopoles was employed throughout. Element field patterns were normalized to the unit cell gain $(2\pi d/\lambda)^{1/2}$ and ten probe current terms were used in Galerkin's procedure. Several numerical results for element patterns and coupling coefficients are presented below for the following element geometry: $a = 0.01 \lambda$, $b = 0.034 \lambda$, $l = 0.25 \lambda$. The separation between the two parallel plates $h = 0.37 \lambda$ and the distance from the element to the cylindrical ground $s = 0.25 \lambda$.

Fig. 4 illustrates the dependence of the element field pattern on the inter-element spacing d/λ . Comparison with the equivalent infinite linear array is also given^[2] (for $d = 0.6 \lambda$). It is observed that all patterns exhibit a substantial drop-off near $\phi = \arcsin(\lambda/d - 1)$. In the linear array case this drop-off is caused by an end-fire grating lobe condition and in the cylindrical array by its quasi-linear counterpart as discussed in [3] for the case of a cylindrical array of axial strip-dipoles. The curves of Fig. 4 also exhibit a ripple in the broadside region, whose amplitude diminishes with closer element spacings and becomes negligible for $d/\lambda = 0.5$. The ripple is due to the interference of the direct single element radiation (with planar element pattern) with the grating lobes of corresponding quasi-linear subarrays excited by the guided creeping wave as discussed in [3].

Fig. 5 illustrates the pattern dependence on the array radius. It is seen that in the shadow region the pattern falls off exponentially which indicates that it is primarily due to a single creeping wave. The ripple in the $\phi = 180^\circ$ region, similarly to that found in the case of conducting cylinder, is a result of the interference of two creeping waves traveling in opposite directions around the cylinder.

Coupling coefficients for the circular and its equivalent infinite linear array are presented in Fig. 6. As expected, in the circular array the coupling coefficients initially follow that of linear array. For elements far from the excited one ($p=0$), the coupling coefficients decrease exponentially which again indicates that the main contribution is primarily due to the creeping wave.

REFERENCES:

1. A. Hessel and B. Tomasic: "Mutual Coupling in Bootlace Lenses", International URSI - Symposium Digest, Munich, W. Germany, 1980.
2. B. Tomasic and A. Hessel: "Linear Phased Array of Coaxially-fed Monopole Elements in a Parallel Plate Guide", IEEE/AP-S Symposium Digest, Albuquerque, New Mexico, May 1982.
3. J.C. Herper, A. Hessel, and B. Tomasic: "Element Pattern of an Axial Dipole in a Cylindrical Phased Array, Part I - Theory, Part II - Element Design & Experiment", to be published in IEEE Transactions on Antennas and Propagation, March 1985.

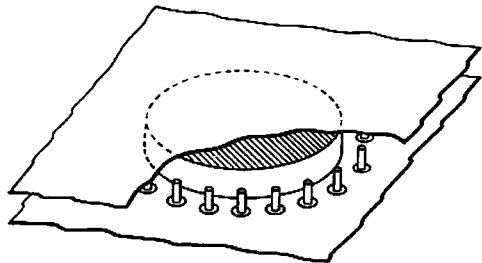


Fig. 1 Circular-ring array in an infinite parallel plate waveguide

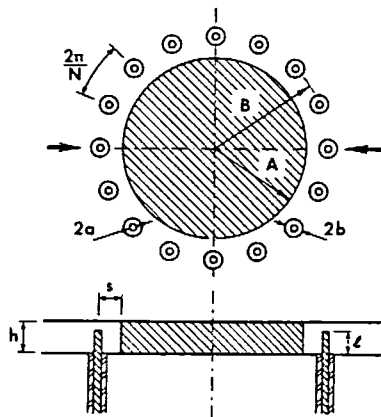


Fig. 2 Top and side view of the array model

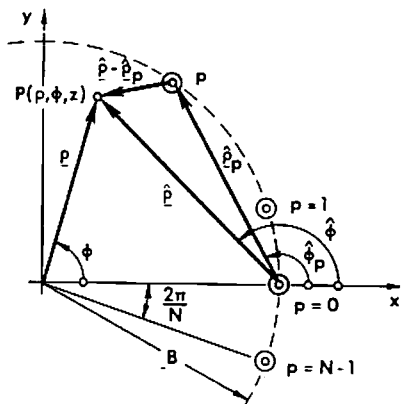


Fig. 3 Array geometry pertaining to evaluation of $E_z(\underline{r};v)$

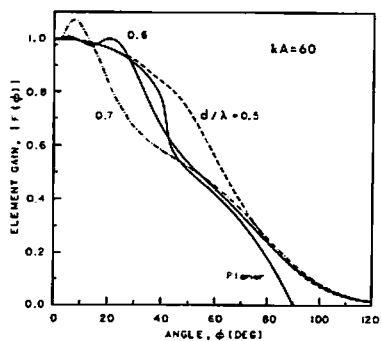


Fig. 4 Element pattern amplitude (linear scale)

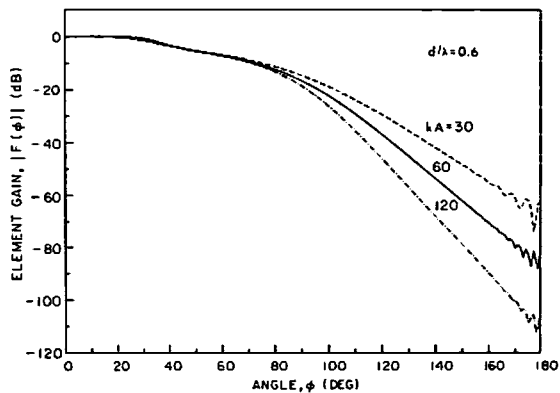


Fig. 4 Element pattern amplitude (log scale)

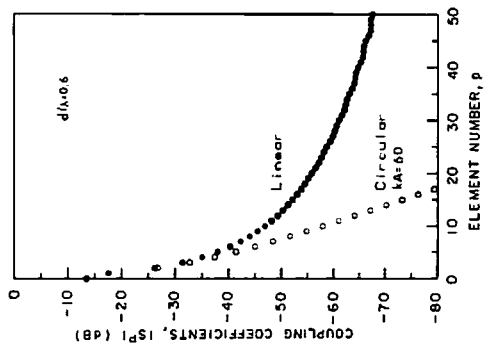


Fig. 6 Coupling coefficients